Magnetism of the *A*-site ordered perovskites $CaCu_3Cr_4O_{12}$ and $LaCu_3Cr_4O_{12}$

Jun Sugiyama,[1,2,*] Hiroshi Nozaki,[1] Izumi Umegaki,[1] Kazutoshi Miwa,[1] Wataru Higemoto,[2] Eduardo J. Ansaldo,[3] Jess H. Brewer,[4,5] Hiroya Sakurai,[6] Masahiko Isobe,[7] Hidenori Takagi,[7] and Martin Månsson[8]

[1]*Toyota Central Research and Development Laboratories Inc., Nagakute, Aichi 480-1192, Japan*
[2]*Advanced Science Research Center, Japan Atomic Energy Agency, Tokai, Ibaraki 319-1195, Japan*
[3]*Department of Physics and Engineering Physics, University of Saskatchewan, Saskatoon, Saskatchewan, Canada S7N 5E2*
[4]*TRIUMF, 4004 Wesbrook Mall, Vancouver, British Columbia, Canada V6T 2A3*
[5]*Department of Physics and Astronomy, University of British Columbia, Vancouver, British Columbia, Canada V6T 1Z1*
[6]*National Institute for Materials Science, Namiki, Tsukuba, Ibaraki 305-0044, Japan*
[7]*Max Planck Institute for Solid State Research, Heisenbergstraße 1, 70569 Stuttgart, Germany*
[8]*Department of Materials Physics, KTH Royal Institute of Technology, SE-16440 Stockholm Kista, Sweden*

(Received 11 September 2017; published 18 January 2018)

The microscopic magnetic nature of the *A*-site ordered chromium perovskites $CaCu_3Cr_4O_{12}$ and $LaCu_3Cr_4O_{12}$ and their solid-solution system, $Ca_{1-x}La_xCu_3Cr_4O_{12}$, with $x = 0.2$, 0.4, and 0.8, has been studied with muon spin rotation and relaxation (μ^+SR) measurements down to 2 K using a powder sample. For $CaCu_3Cr_4O_{12}$, μ^+SR revealed the formation of static antiferromagnetic (AF) order below 122 K ($=T_N$), although magnetization measurements showed a very small change at T_N. Analyses of the internal magnetic field H_{int} at the muon sites, predicted with first-principles calculations, suggested *G*-type AF order as a ground state. For $LaCu_3Cr_4O_{12}$ with $T_N = 225$ K, μ^+SR also supported the presence of a *G*-type AF ordered state, which was recently proposed based on neutron diffraction measurements. However, the ordered Cr moments were found to change the direction at around 10 K. For $Ca_{1-x}La_xCu_3Cr_4O_{12}$, both T_N and H_{int} at 2 K increase monotonically with x.

DOI: 10.1103/PhysRevB.97.024416

I. INTRODUCTION

In searches for a novel eccentric phase, e.g., a quantum critical phase (QCP), near the boundary between an antiferromagnetic (AF) ground state and a Kondo-like state, a huge number of solid-solution systems have been investigated as a function of spin density in the lattice, particularly for f-electron systems [1]. However, it is challenging to find such phases in d-electron oxide systems because of an overlap of the d orbitals with the p orbital of oxygen.

Recently, a solid-solution system between two *A*-site ordered chromium oxide perovskites, $ACu_3Cr_4O_{12}$, with $A =$ Ca and La, has been proposed as a possible candidate in the search for a QCP. This is because $CaCu_3Cr_4O_{12}$ was reported to be a Pauli paramagnetic metal [2], and a related compound, $CaCu_3Ru_4O_{12}$, exhibits heavy-fermion behavior based on magnetic susceptibility χ and heat capacity C_p measurements [3], whereas $LaCu_3Cr_4O_{12}$ was found to be an AF metal by recent resistivity and muon spin rotation (μ^+SR) measurements [4].

Note that in the $AA'_3Cr_4O_{12}$ ($=A_{1/4}A'_{3/4}CrO_3$) lattice, due to the tilting of CrO_6 octahedra, the coordination number of A' is reduced from 12 to 4, leading to a square-planar coordination. As a result, we have a $AA'_3Cr_4O_{12}$ structure (see Fig. 1) in which the coordination numbers are 12, 4, and 6 for A, A', and B, respectively [5,6]. Such a perovskite is called an *A*-site ordered chromium perovskite. Here, either Cu^{2+} or Mn^{3+} ions prefer to occupy the A' site because of a Jahn-Teller effect. In fact, the first $AA'_3B_4O_{12}$ compounds were found in 2002: $ACu_3Ti_4O_{12}$ and $ACu_3Ru_4O_{12}$ [3,5,7].

Particularly for $ACu_3Cr_4O_{12}$, with $A =$ Ca and La, Cr ions are in a 4+ state with $S = 1(t_{2g}^2)$ for $CaCu_3Cr_4O_{12}$ versus a mixed-valence state (3.75+) between $S = 1(t_{2g}^2)$ and $S = 3/2(t_{2g}^3)$ for $LaCu_3Cr_4O_{12}$. This means that the orbital degree of freedom is partially suppressed in $LaCu_3Cr_4O_{12}$.

Historically, the first $ACu_3Cr_4O_{12}$ compound synthesized was $CaCu_3Cr_4O_{12}$, using a high-pressure technique at 1100 °C under 60 kbar (=6 GPa) in 2003 [2]. Despite its metallic conductivity, the magnetic ground state of $CaCu_3Cr_4O_{12}$ has been predicted to be a ferrimagnet with ordered Cr and Cu moments by first-principles calculations [8,9]. In addition, magnetization measurements revealed the presence of a small magnetic anomaly at around 150 K. However, due to the presence of a $CuCr_2O_4$ impurity phase with $T_{ferri} = 150$ K, the magnetic ground state of $CaCu_3Cr_4O_{12}$ is still not clear.

Compounds with trivalent ions at the A site have been also synthesized by a high-pressure technique. The first such compound, $LaCu_3Cr_4O_{12}$, was found in 2012 by Isobe and Sakurai [10] and independently in 2014 by Zhang and coworkers [11]. Magnetization measurements revealed the presence of a sharp magnetic transition at 225 K (Fig. 2), implying the appearance of a spin-singlet-like state. Nevertheless, μ^+SR measurements demonstrated the presence of static magnetic order in $LaCu_3Cr_4O_{12}$ [4]. This clearly indicates the importance of μ^+SR for studying magnetic ground states of complex

*e0589@mosk.tytlabs.co.jp

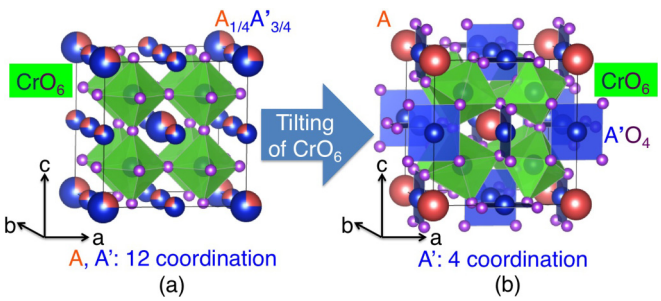

FIG. 1. The crystal structure of (a) a regular perovskite, $A_{1/4}A'_{3/4}CrO_3$, and (b) an A-site ordered perovskite, $AA'_3Cr_4O_{12}$.

oxides, as already shown for other chromium compounds [12–19].

Returning to a solid-solution system between $CaCu_3Cr_4O_{12}$ and $LaCu_3Cr_4O_{12}$, very recently, $Ca_{1-x}La_xCu_3Cr_4O_{12}$ was successfully synthesized using a high-pressure technique in the whole x range between 0 and 1 (see Fig. 2). Nevertheless, the QCP phase has not been found in this system. This raises a question about the magnetic ground state of $CaCu_3Cr_4O_{12}$. We have therefore investigated the magnetic properties of $CaCu_3Cr_4O_{12}$ and $Ca_{1-x}La_xCu_3Cr_4O_{12}$ with μ^+SR because μ^+SR provides microscopic magnetic information about a sample due to its unique localization and high time resolution [20,21]. Furthermore, even for a sample consisting of multiple magnetic phases, μ^+SR can often extract the volume fraction of each magnetic phase. Here, we report an AF ground state for $CaCu_3Cr_4O_{12}$ and show that the $Ca_{1-x}La_xCu_3Cr_4O_{12}$ system is unfortunately not a playground for studying QCP.

II. EXPERIMENT

Polycrystalline samples of $CaCu_3Cr_4O_{12}$, $LaCu_3Cr_4O_{12}$, and $Ca_{1-x}La_xCu_3Cr_4O_{12}$ were synthesized from stoichiometric mixtures of CaO, La_2O_3, CuO, Cr_2O_3, and CrO_2 at 1200 °C under a pressure of 7.7 GPa for 1–2 h. The details of the synthesis have been described elsewhere [10]. Powder x-ray diffraction (XRD) analyses showed that the samples were almost single phase with a small (less than 2 wt %) CrO_2 impurity.

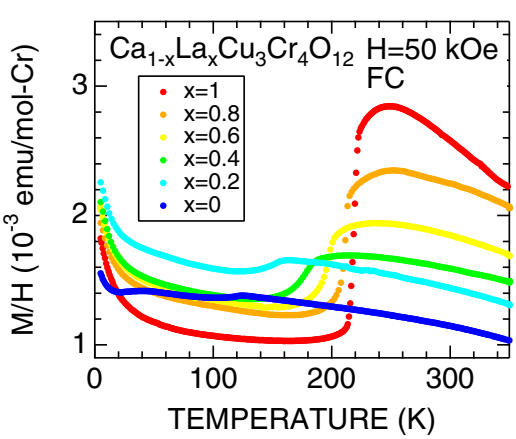

FIG. 2. Temperature dependence of the magnetic susceptibility ($\chi = M/H$) of $Ca_{1-x}La_xCu_3Cr_4O_{12}$ measured at $H = 50$ kOe.

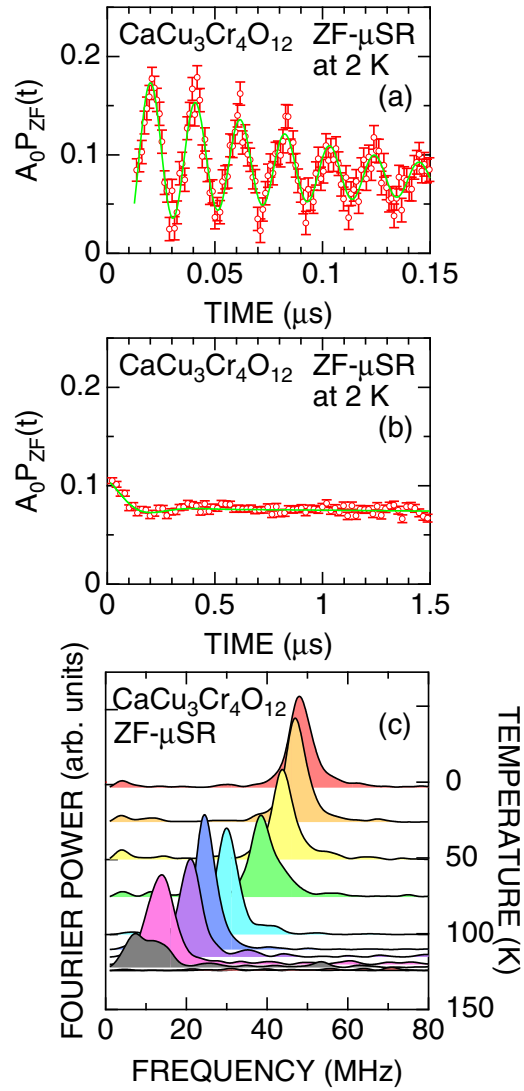

FIG. 3. (a) The ZF-μ^+SR time spectrum for $CaCu_3Cr_4O_{12}$ at 1.8 K, displayed with 1.1-ns time bins in the early time domain ($t < 0.15$ μs), (b) the same spectrum displayed with 20-ns time bins for $T < 1.5$ μs, and (c) the temperature variation of the frequency spectrum. Solid lines in (a) and (b) represent the fit using Eq. (1). In (c), the Fourier transform was performed in the time range from 0 to 0.35 μs.

The μ^+SR spectra were measured on the M20 surface muon beam line using the LAMPF spectrometer at TRIUMF in Canada. Each approximately 200-mg powder sample was placed in a 1×1 cm^2 square envelope made from 0.05-mm-thick aluminized Mylar tape in order to minimize the signal from the envelope. The envelope was attached to a low-background sample holder in a liquid-He flow-type cryostat for measurements in the T range between 2 and 250 K. The experimental techniques are described in more detail elsewhere [20,21].

III. RESULTS

A. $CaCu_3Cr_4O_{12}$

Figures 3(a) and 3(b) show the μ^+SR time spectrum obtained in zero magnetic field (ZF) at the lowest temperature

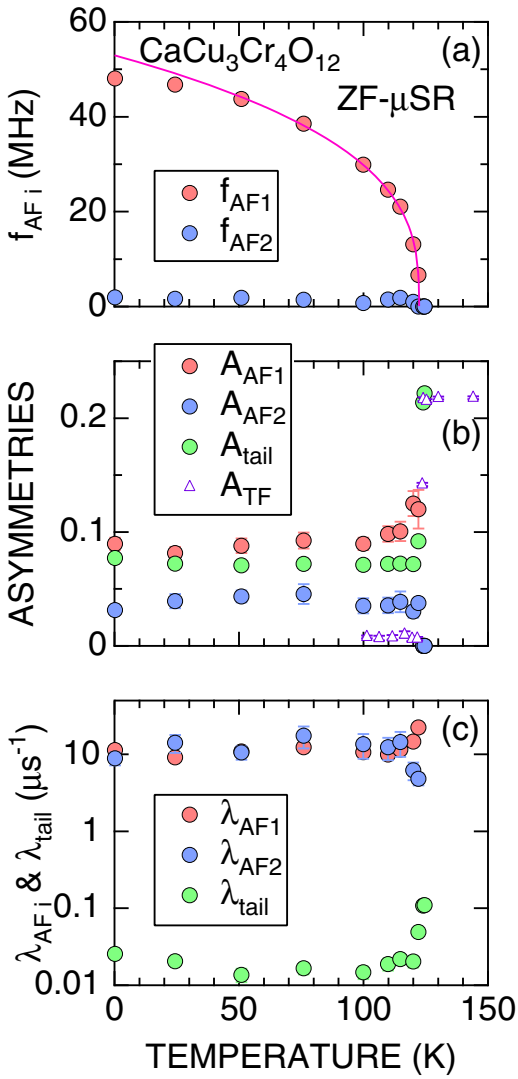

FIG. 4. The temperature dependences of (a) the muon Larmor frequencies ($f_{\mathrm{AF_1}}$ and $f_{\mathrm{AF_2}}$), (b) the asymmetries ($A_{\mathrm{AF_1}}$, $A_{\mathrm{AF_2}}$, A_{tail}, and A_{TF}), and (c) the relaxation rates ($\lambda_{\mathrm{AF_1}}$, $\lambda_{\mathrm{AF_2}}$, and λ_{tail}) for $CaCu_3Cr_4O_{12}$. The data were obtained by fitting the ZF spectrum with Eq. (1). In (a), the solid line on the $f_{\mathrm{AF_1}}(T)$ curve is a power-law fit at temperatures between 50 and 122 K. In (b), A_{TF} is the weak transverse field (TF) asymmetry, which is roughly proportional to the volume fraction of paramagnetic phases in a sample. Here, TF means the magnetic field is perpendicular to the initial muon spin polarization, and "weak" means that the TF (50 Oe) is very small compared with the internal AF field.

measured (1.8 K). At early times ($t < 0.15\,\mu$s), the spectrum exhibits a clear muon spin oscillation, indicating the formation of quasistatic magnetic order in $CaCu_3Cr_4O_{12}$. Moreover, the same spectrum plotted for $t < 1.5\,\mu$s shows a strongly damped oscillation with a first minimum at around $t = 0.2\,\mu$s. This suggests the presence of two magnetically different muon sites in the lattice. Note that the precession signal in Fig. 3(a) is averaged out in Fig. 3(b) due to its more coarsely packed bins (20 ns).

In fact, there are two distinct peaks in the Fourier transform frequency spectrum at 1.8 K: a major component at around

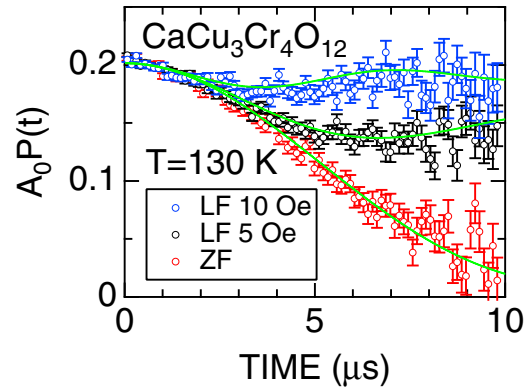

FIG. 5. The ZF- and LF-μ^+SR spectra for $CaCu_3Cr_4O_{12}$ at 130 K. Solid lines represent the fit using a dynamic Gaussian Kubo-Toyabe function.

47 MHz and a minor component at around 2 MHz [see Fig. 3(c) and Sec. V]. Furthermore, as the temperature increases, the frequency of the major peak decreases, and the oscillatory signal finally disappears at around 125 K, while that of the minor peak looks roughly temperature independent but also becomes undetectable above 125 K.

Therefore, the ZF-μ^+SR time spectrum was fitted by a combination of two exponentially relaxing cosine oscillations for the quasistatic AF internal fields and an exponentially relaxing nonoscillatory signal for the "1/3 tail" signal caused by fluctuations in the field component initially parallel to the initial muon spin polarization $\boldsymbol{P}_\mu(0)$:

$$A_0\, P_{\mathrm{ZF}}(t) = \sum_{i=1}^{n} A_{\mathrm{AF}_i} e^{-\lambda_{\mathrm{AF}_i} t} \cos\left(\omega_{\mathrm{AF}_i} t + \phi_{\mathrm{AF}_i}\right) + A_{\mathrm{tail}} e^{-\lambda_{\mathrm{tail}} t}\,. \tag{1}$$

Here, A_0 is the initial asymmetry, $n = 2$ is the number of oscillatory signals, $P_{\mathrm{ZF}}(t)$ is the muon spin depolarization function in ZF, A_{AF_i} and A_{tail} are the asymmetries associated with the three signals, $f_{\mathrm{AF}_i}(\equiv \omega_{\mathrm{AF}_i}/2\pi)$ are the muon Larmor frequencies corresponding to the quasistatic internal AF fields, λ_{AF_i} and λ_{tail} are their exponential relaxation rates, and ϕ_{AF_i} are the initial phases. Note that the initial phase of the minor component was fixed as zero; that is, $\phi_{\mathrm{AF}_2} = 0$ due to the difficulty to estimate ϕ_{AF_2} from the spectrum having only one minimum [see Fig. 3(b)].

Figure 4 shows the temperature dependences of the μ^+SR parameters obtained by fitting the ZF-μ^+SR spectrum with Eq. (1). The $f_{\mathrm{AF_1}}(T)$ curve shows a typical order-parameter-like temperature dependence. A power-law fit, $f/f_0 = [(T_{\mathrm{N}} - T)/T_{\mathrm{N}}]^{\beta}$, to $f_{\mathrm{AF_1}}(T)$ in the temperature range between 50 and 122 K provides $f_0 = 53.0 \pm 0.7$ MHz, $T_{\mathrm{N}} = 122.32 \pm 0.07$ K, and $\beta = 0.338 \pm 0.009$. This implies a three-dimensional nature of the AF order in $CaCu_3Cr_4O_{12}$, although we need more accurate data below the vicinity of T_{N}.

On the other hand, $f_{\mathrm{AF_2}}$ is almost temperature independent up to T_{N}. However, since the $A_{\mathrm{AF_2}}$ signal also disappears at T_{N}, that signal must come not from a magnetic impurity phase but from a second muon site in the lattice, at which the internal magnetic field H_{int} is very small compared with H_{int} at the site for the $A_{\mathrm{AF_1}}$ signal.

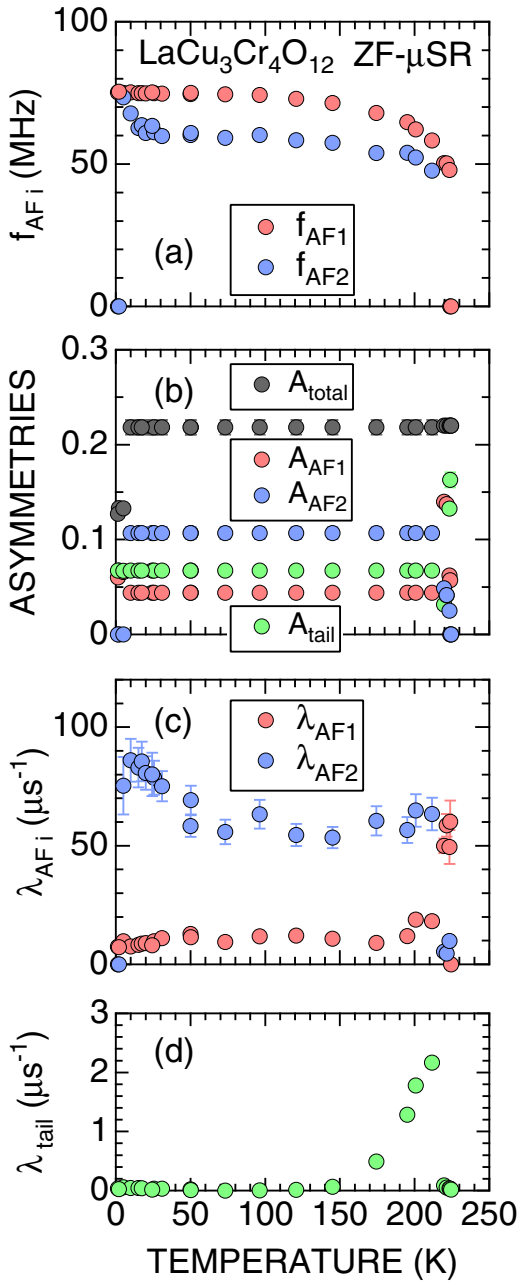

FIG. 6. The temperature dependences of (a) the muon oscillation frequencies (f_{AF_1} and f_{AF_2}), (b) the asymmetries (A_{AF_1}, A_{AF_2}, A_{tail}, and their sum A_{total}), (c) the exponential relaxation rates of the precession signals (λ_{AF_1} and λ_{AF_2}), and (d) the exponential relaxation rate of the "tail" signal (λ_{tail}) for $LaCu_3Cr_4O_{12}$. The data were obtained by fitting the ZF-μ^+SR spectrum to Eq. (1).

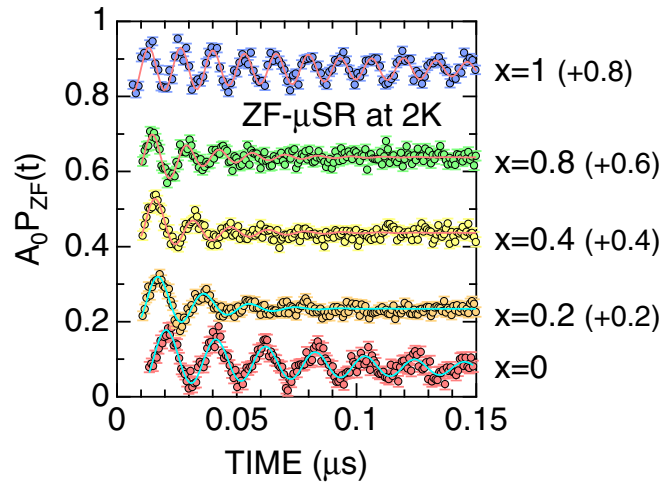

FIG. 7. The ZF-μ^+SR spectra for $Ca_{1-x}La_xCu_3Cr_4O_{12}$, with $x = 0, 0.2, 0.4, 0.8$, and 1, obtained at 2 K. Each spectrum is shifted upward by 0.2 for clarity of display. Solid lines represent the fit result using Eq. (1).

The value of ϕ_{AF_1} is $10^\circ \pm 3^\circ$ at 1.8 K, suggesting a commensurate AF order magnetic ground state for $CaCu_3Cr_4O_{12}$. In addition, although ϕ_{AF_1} changes with temperature, $|\phi_{AF_1}| \leqslant 20^\circ$ below T_N (not shown).

The three asymmetries (A_{AF_1}, A_{AF_2}, and A_{tail}) and their relaxation rates (λ_{AF_1}, λ_{AF_2}, and λ_{tail}) are roughly temperature independent except in the vicinity of T_N, as expected. At T_N, the $A_{tail}(T)$ curve shows an abrupt change because of the sudden increase in the paramagnetic phase with increasing temperature. In Fig. 4(b), the temperature dependence of the weak transverse field (WTF) asymmetry A_{TF} [where "transverse" means the applied field is perpendicular to $\boldsymbol{P}_\mu(0)$ and "weak" means that said field is very small compared with H_{int} caused by AF order] is also plotted for comparison. Here, the WTF-μ^+SR spectra were fitted by

$$A_0\, P_{TF}(t) = A_{TF} e^{-\lambda_{TF} t} \cos(\omega_{TF} t + \phi) + A_M e^{-\lambda_M t}, \quad (2)$$

where A_{TF} and A_M are, respectively,0 the asymmetry of the precession signal due to the applied WTF and that of the nonoscillatory relaxing signal caused by localized magnetic moments. Since A_{TF} is proportional to the volume fraction of paramagnetic phases in a sample, a steplike change at T_N indicates a sharp AF transition at T_N in the whole sample.

Above T_N, the ZF-μ^+SR spectrum exhibits a slow relaxation by random fields due to nuclear magnetic moments. Figure 5 shows ZF and two longitudinal field (LF) μ^+SR spectra measured at 130 K. [Here, LF means the field parallel to $\boldsymbol{P}_\mu(0)$, which suppresses relaxation caused by nuclear magnetism.] Fitting the ZF and LF spectra with a dynamic Gaussian Kubo-Toyabe function [22,23], we obtain the field distribution width ($\Delta = 0.143 \pm 0.002\ \mu s^{-1} \Rightarrow \langle B_{dip}^2 \rangle^{1/2} = 1.68 \pm 0.02$ Oe) and field fluctuation rate ($\nu = 0.011 \pm 0.008\ \mu s^{-1}$). This means that the nuclear magnetic fields are almost static at 130 K, while both Cr and Cu moments are thermally fluctuating too rapidly for their fields to be effective in the μ^+SR time window.

B. $LaCu_3Cr_4O_{12}$

For $LaCu_3Cr_4O_{12}$, a clear muon spin oscillation signal was also observed below $T_N = 225$ K. A preliminary result was reported in Ref. [4]; those ZF-μ^+SR data, together with new data below 30 K, were fitted using Eq. (1). As the temperature increases from 2 K, the number of the oscillatory signals n changes from 1 to 2 at $\sim$10 K and then decreases to 1 again as $T \to T_N$ from below. In addition, since a recent neutron scattering measurement [24] shows a commensurate

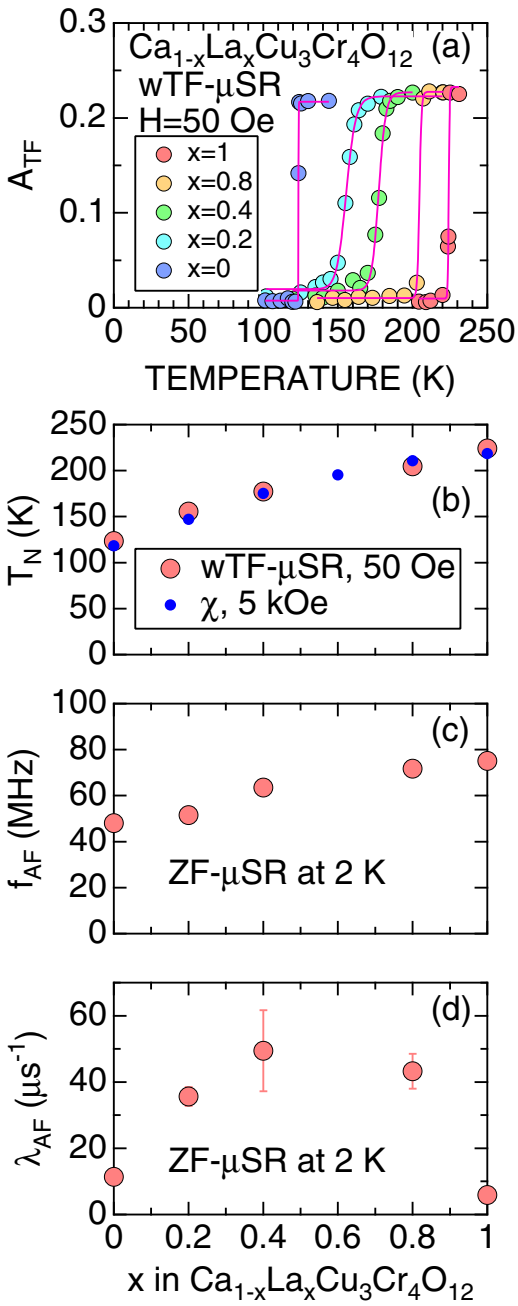

FIG. 8. (a) The temperature dependence of the weak transverse field asymmetry $A_{\rm TF}$ for $Ca_{1-x}La_xCu_3Cr_4O_{12}$, with $x = 0$, 0.2, 0.4, 0.8, and 1, (b) the antiferromagnetic transition temperature $T_{\rm N}$, (c) the ZF muon-spin oscillation frequency at 2 K $f_{\rm AF}$, and (d) the exponential relaxation rate of the ZF $f_{\rm AF}$ signal as a function of x. In (a), the data were obtained by fitting the WTF-μ^+SR spectrum with Eq. (2).

AF order at 5 and 200 K, $\phi_{{\rm AF}_i}$ was fixed to zero in the whole temperature range measured. Furthermore, we used a global fit with common values of $A_{{\rm AF}_i}$ and $A_{\rm tail}$ between 10 and 219 K, giving $A_{{\rm AF}_1} = 0.0440 \pm 0.0013$, $A_{{\rm AF}_2} = 0.1069 \pm 0.0063$, and $A_{\rm tail} = 0.0673 \pm 0.00010$.

Figure 6 shows the temperature dependences of the μ^+SR parameters for $LaCu_3Cr_4O_{12}$. Of the two frequencies, the $f_{{\rm AF}_1}(T)$ curve exhibits an order-parameter-like temperature dependence. The very abrupt change of $f_{{\rm AF}_1}$ at $T_{\rm N}$ implies that the AF transition is not continuous but discontinuous. In fact, since a thermal hysteresis is clearly observed in the $\chi(T)$ curves measured on cooling and on heating, the AF transition is assumed to be accompanied by a discontinuous structural phase transition.

TABLE I. Calculated structural parameters of $CaCu_3Cr_4O_{12}$ and $LaCu_3Cr_4O_{12}$. Both compounds have cubic symmetry with space group $Im\bar{3}$ (No. 204). The lattice constant of the former is $a = 7.306$ Å, whereas the latter has $a = 7.382$ Å.

	Site	x	y	z
Ca	2*a*	0	0	0
Cu	6*b*	0	1/2	1/2
Cr	8*c*	1/4	1/4	1/4
O	24*g*	0	0.3023	0.1819
μ^+	24*g*	0	0.7355	0.4526
La	2*a*	0	0	0
Cu	6*b*	0	1/2	1/2
Cr	8*c*	1/4	1/4	1/4
O	24*g*	0	0.3022	0.1819
μ^+	12*e*	0.2439	0	1/2

It should be noted that below 10 K the $A_{{\rm AF}_2}$ signal disappears and the total symmetry ($A_{\rm total} \equiv A_{{\rm AF}_1} + A_{{\rm AF}_2} + A_{\rm tail}$) becomes rather small compared with that above 10 K. Since $LaCu_3Cr_4O_{12}$ is metallic down to 2 K, the formation of muonium states is unlikely to explain such a decrease in $A_{\rm total}$. From the $f_{{\rm AF}_1}(T)$ and $f_{{\rm AF}_2}(T)$ curves, the $A_{{\rm AF}_2}$ signal looks to be merged into the $A_{{\rm AF}_1}$ signal below 10 K. However, in order to explain the sudden decrease in $A_{\rm total}$, we need to assume that $f_{{\rm AF}_1} = f_{{\rm AF}_2}$ but $\lambda_{{\rm AF}_2} \to \infty$ below 10 K. Such an assumption naturally leads to a very inhomogeneous internal magnetic field in the lattice. Therefore, it is reasonable to assume that the $A_{{\rm AF}_2}$ signal disappears below 10 K.

On the other hand, at temperatures between 10 and 219 K, $A_{{\rm AF}_2} \sim 2.5 A_{{\rm AF}_1}$, although the $A_{{\rm AF}_2}$ signal is heavily damped in the whole temperature range below $T_{\rm N}$. This implies that the muons responsible for the $A_{{\rm AF}_2}$ signal *see* an internal magnetic field with a broad field distribution. The muon sites and the internal magnetic field at each site will be discussed in Sec. IV.

C. $Ca_{1-x}La_xCu_3Cr_4O_{12}$

Figure 7 shows the ZF-μ^+SR spectra at 2 K for $Ca_{1-x}La_xCu_3Cr_4O_{12}$ samples with $x = 0$, 0.2, 0.4, 0.8, and 1. A muon spin oscillation signal is clearly observed for each spectrum, although said signals are more rapidly damped for the solid-solution samples ($0 < x < 1$) than in the pure samples ($x = 0$ and $x = 1$). This means that, although each sample with $0 < x < 1$ is in a static AF ordered phase at 2 K, the internal AF field is less homogeneous than those in the pure samples.

In addition to the ZF-μ^+SR data, WTF measurements demonstrate the presence of a sharp magnetic transition in the temperature range between 225 and 130 K for each sample [see Fig. 8(a)]. Assuming that $T_{\rm N}$ is the temperature at which $A_{\rm TF}(T_{\rm N})/A_0 = 0.5$, $T_{\rm N}$ is found to increase monotonically with La content x, and the $T_{\rm N}$ determined by WTF μ^+SR is almost

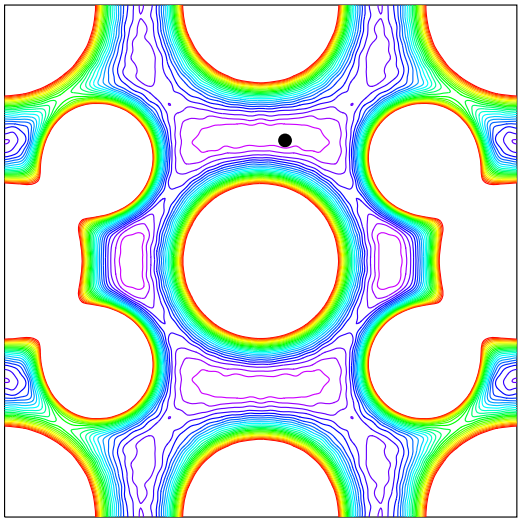

FIG. 9. Contour plots of the electrostatic potential in the (001) plane for $CaCu_3Cr_4O_{12}$. The contour spacing is 0.2 eV, and the lines are omitted where the potential exceeds 5 eV.

equivalent to that determined by magnetization measurements at $H = 50$ kOe [Fig. 8(b)].

Based on fits of the ZF-μ^+SR spectra for the samples with $x = 0.2$, 0.4, and 0.8 using Eq. (1) with $n = 1$, f_{AF} at 2 K also increases monotonically with x. However, the $\lambda_{AF}(x)$ curve shows a broad maximum at $x \sim 0.5$, indicating an increase in the randomness of the internal AF field with x up to 0.5. Here, the results for the pure samples correspond to the AF_1 signal, i.e., f_{AF_1} and λ_{AF_1}. This also suggests that the muon sites are not drastically changing with x. Returning to the original motivation for searching for an eccentric phase, it is clear that such a phase does not exist in the solid-solution system between $CaCu_3Cr_4O_{12}$ and $LaCu_3Cr_4O_{12}$.

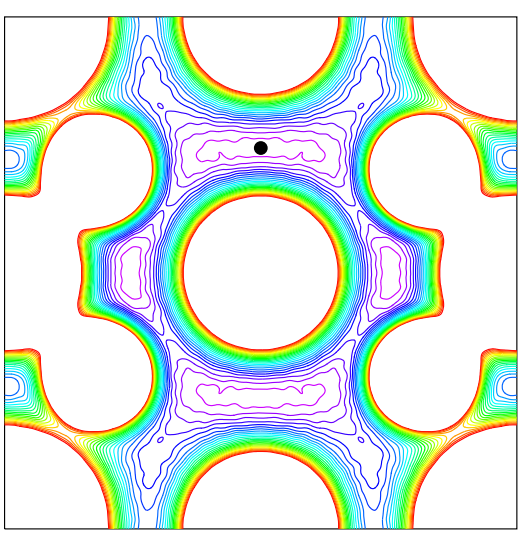

FIG. 10. Contour plots of the electrostatic potential in the (001) plane for $LaCu_3Cr_4O_{12}$. The contour spacing is 0.2 eV, and the lines are omitted where the potential exceeds 5 eV.

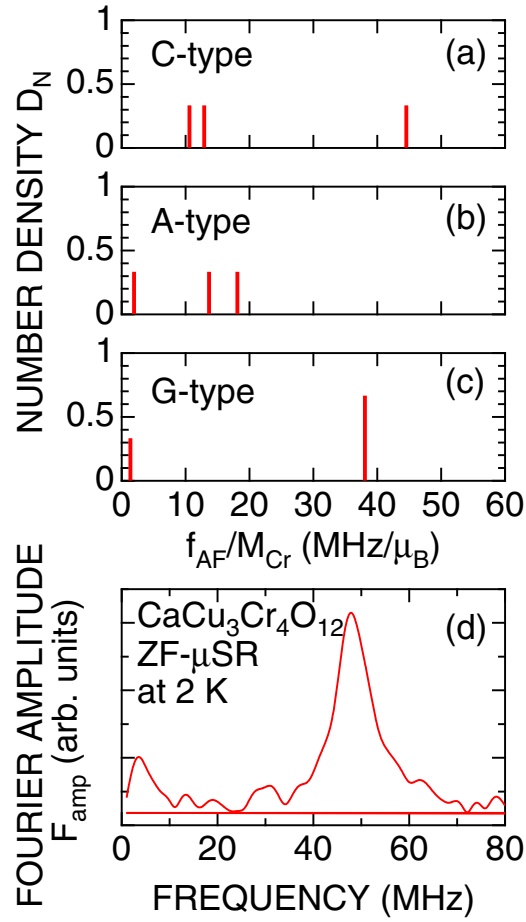

FIG. 11. The distribution of the internal magnetic field H_{int} at the muon sites, i.e., the number density D_N of H_{int}, for (a) C-type, (b) A-type, and (c) G-type AF ordered states and (d) the Fourier amplitude spectrum at 2 K in $CaCu_3Cr_4O_{12}$. In (a)–(c), the ordered Cr moments $\boldsymbol{M}_{Cr}$ are assumed to be parallel or antiparallel to the c axis. For the C-type AF ordered state, $\boldsymbol{M}_{Cr}$ aligns AF in the ab plane but ferromagnetically (FM) along the c axis. For A-type AF, $\boldsymbol{M}_{Cr}$ aligns FM in the ab plane but AF along the c axis. For G-type AF, $\boldsymbol{M}_{Cr}$ aligns AF in the ab plane and along the c axis. Note that there are 24 crystallographically equivalent muon sites in the lattice (see Table I), which provide $24H_{int_i}$, with $i = 1$–24. In (a), we obtained $H_{int} = 10.6\,\mathrm{MHz}/\mu_B$ for eight sites, $12.9\,\mathrm{MHz}/\mu_B$ for eight sites, and $44.5\,\mathrm{MHz}/\mu_B$ for eight sites. Thus, D_N of each H_{int} is 1/3 (=8/24).

IV. DISCUSSION

A. Muon sites

In order to speculate about the AF spin structure in $CaCu_3Cr_4O_{12}$ and $LaCu_3Cr_4O_{12}$, the muon sites in the lattice were predicted by first-principles calculations [25] based on density-functional theory (DFT) [26,27] with the generalized gradient approximation (GGA) [28,29]. The results obtained for the two compounds are summarized in Table I and Figs. 9 and 10. It is found that the μ^+s is located in the vicinity of the O^{2-} ions in the CuO_4 square plane, leading to 24 (12) crystallographically equivalent sites in the $CaCu_3Cr_4O_{12}$ ($LaCu_3Cr_4O_{12}$) lattice.

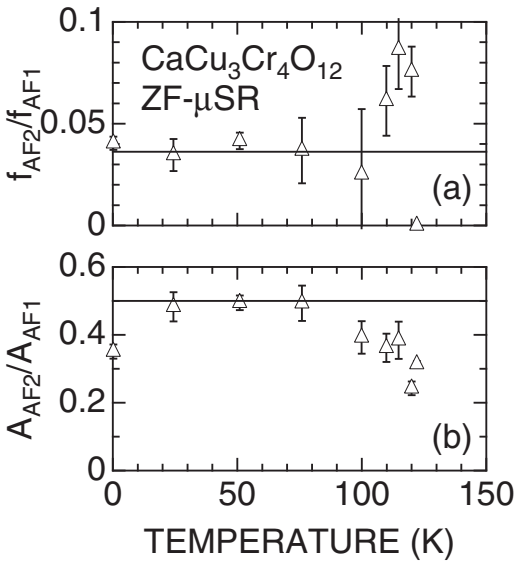

FIG. 12. The temperature dependences of (a) f_{AF_2}/f_{AF_1} and (b) A_{AF_2}/A_{AF_1} for $CaCu_3Cr_4O_{12}$ calculated from the data shown in Fig. 4. Solid lines show the prediction for the *G*-type AF ordered state.

B. AF structure for $CaCu_3Cr_4O_{12}$

Here, we assumed that only Cr moments are responsible for AF order and the Cu moments are random even at 2 K, as proposed for $LaCu_3Cr_4O_{12}$ [24] and as reported for $CaCu_3Ru_4O_{12}$ [30]. Using the muon sites listed in Table I, the distribution of the internal magnetic field H_{int} at the muon sites was estimated by dipole field calculations with DIPELEC [31] for the three AF ordered states, i.e., *C*-type, *A*-type, and *G*-type AF ordered states [see Figs. 11(a)–11(c)]. Although there are 24 crystallographically equivalent sites in the lattice, two or three magnetically different sites are found to be present in the AF ordered states.

Making a comparison with the ZF-μ^+SR frequency spectrum obtained at 2 K [Fig. 11(d)], *G*-type AF order is the most acceptable ground state for $CaCu_3Cr_4O_{12}$. In fact, except in the vicinity of T_N, the measured f_{AF_2}/f_{AF_1} is very close to the predicted frequency ratio, 0.036 [Fig. 12(a)]. Furthermore, the fact that $A_{AF_2}/A_{AF_1} = 0.44 \pm 0.04$ for the data below 100 K [Fig. 12(b)] is very consistent with the *G*-type AF ordered state; namely, the predicted amplitude ratio between the two frequencies is 0.5. Therefore, not only the measured f_{AF_i} but also the measured A_{AF_i} support *G*-type AF order in $CaCu_3Cr_4O_{12}$.

The ordered magnetic moment of Cr ions M_{Cr} is estimated to be $1.33\mu_B \pm 0.07\mu_B$, which is about 67% of the spin-only magnetic moment for Cr^{4+} ions with $S = 1$ (t_{2g}^2). This is also reasonable for the metallic nature of $CaCu_3Cr_4O_{12}$ even below T_N.

C. *G*-type AF structure for $LaCu_3Cr_4O_{12}$

For $LaCu_3Cr_4O_{12}$, a neutron diffraction pattern was measured at 5, 200, 250, and 300 K [24]. Analysis of the magnetic peaks suggested the formation of a *G*-type AF order at 5 K with the AF ordered moment of Cr $M_{Cr}^{neutron} = 1.60\mu_B \pm 0.01\mu_B$ but no moments at Cu ions. Using the proposed AF model

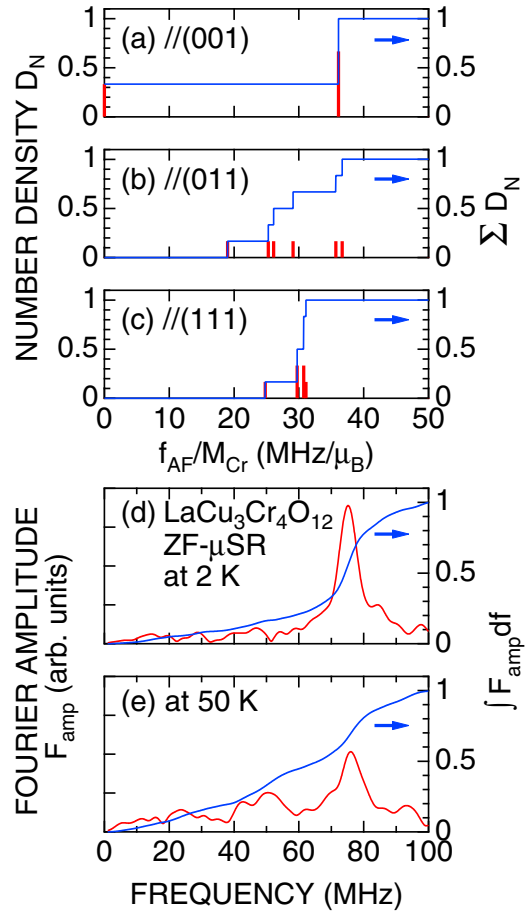

FIG. 13. The distribution of the internal magnetic field H_{int} at the muon sites, i.e., the number density D_N of H_{int}, for *G*-type AF order with (a) $\boldsymbol{M}_{Cr} \parallel (001)$, (b) $\boldsymbol{M}_{Cr} \parallel (011)$, and (c) $\boldsymbol{M}_{Cr} \parallel (111)$ and the Fourier amplitude spectrum (d) at 2 K and (e) at 50 K in $LaCu_3Cr_4O_{12}$. Note that there are 12 crystallographically equivalent muon sites in the lattice (see Table I). Blue solid lines in (a)–(c) represent $\sum_{i=1}^{12} D_{N_i}$, while those in (d) and (e) represent the integrated Fourier amplitude $\int F_{amp} df$.

together with the muon site predicted by DFT calculations, Fig. 13 shows the distribution of H_{int} with $\boldsymbol{M}_{Cr} \parallel (001)$, (011), and (111). Comparison with the ZF-μ^+SR frequency spectrum at 2 K [Fig. 13(d)] confirms that the *G*-type AF order with $\boldsymbol{M}_{Cr} \parallel (001)$ is the ground state. The fact that $D_N = 1/3$ for the signal with $f_{AF} = 0$ is consistent with the missing asymmetry below 10 K [Fig. 6(b)].

On the other hand, a second oscillatory (AF_2) signal appears at temperatures above 10 K with $A_{AF_2}/A_{AF_1} = 2.4 \pm 0.2$. Moreover, $f_{AF_2}/f_{AF_1} = 0.81 \pm 0.02$ in the temperature range between 25 and 219 K. For the *G*-type AF order with $\boldsymbol{M}_{Cr} \parallel (011)$, six different sites with different values of H_{int} are predicted to appear with the same probability, i.e., 1/6. The ratios of D_N and f_{AF}/M_{Cr} between the signals with the four lower frequencies and the higher two are 2 and 0.69, respectively. This suggests that $\boldsymbol{M}_{Cr}$ is canted above 10 K but aligns along the principal axis below 10 K.

In the previous μ^+SR study on $LaCu_3Cr_4O_{12}$ [4], we proposed the formation of an incommensurate (IC) AF phase below T_N and the presence of a transition into a commensurate

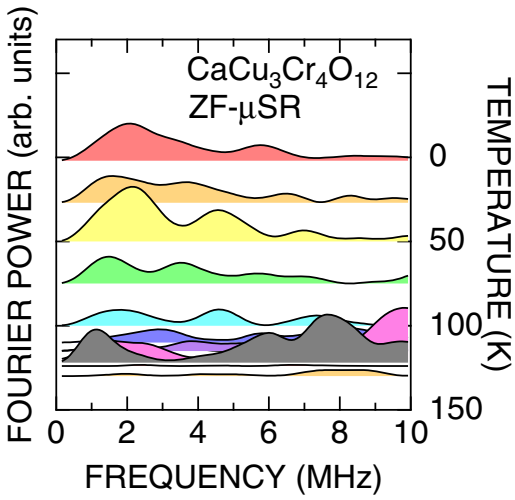

FIG. 14. The temperature variation of the Fourier transform frequency spectrum from the ZF-μ^+SR time spectrum for $CaCu_3Cr_4O_{12}$. The Fourier transform was performed in the time range from 0 to 5 μs.

(C) AF phase below 25 K based on the wide distribution in $H_{\rm int}$. However, considering the absence of IC magnetic Bragg peaks in the recent neutron result [24], a C-AF spin structure mentioned above, i.e., the canted G-type AF, is more reasonable for the magnetic structure of the phase below $T_{\rm N}$.

Since $f_{\rm AF_1} = 75.4$ MHz at 2 K and 75.0 MHz at 50 K [Fig. 6(a)], $M_{\rm Cr}$ is estimated to be 2.1 $\mu_{\rm B}$ at both 2 and 50 K, which is about 93% of the spin-only magnetic moment for $Cr^{3.75+}$ ions. This would not be consistent with the metallic nature of $LaCu_3Cr_4O_{12}$ even below $T_{\rm N}$. In fact, it should be noted that $M_{\rm Cr}$ is 31% higher than $M_{\rm Cr}^{\rm neutron}$, although $M_{\rm Cr}^{\mu\rm SR}$ is comparable to $M_{\rm Cr}^{\rm neutron}$ for materials with static AF order [14,32,33]. This leads to questions on the proposed AF spin structure, the magnitude and direction of $M_{\rm Cr}^{\rm neutron}$, the absence of $M_{\rm Cu}$, and/or the muon site(s). In order to further clarify the AF spin structure, we need to measure and analyze several neutron diffraction patterns below $T_{\rm N}$.

V. SUMMARY

We have measured μ^+SR spectra for powder samples of $CaCu_3Cr_4O_{12}$, $LaCu_3Cr_4O_{12}$, and their solid-solution system, mainly in zero external field (ZF). $CaCu_3Cr_4O_{12}$ was found to enter into a G-type AF ordered state below 122 K ($=T_{\rm N}$), despite only a slight change in magnetization measurements. Assuming that the Cu moments are not ordered down to the lowest temperature measured, the ordered magnetic moment of Cr ions $\boldsymbol{M}_{\rm Cr}$ was found to be parallel to the principal axis, and the magnitude was estimated as $1.33\mu_{\rm B} \pm 0.07\mu_{\rm B}$ at 2 K.

For $LaCu_3Cr_4O_{12}$ with $T_{\rm N} = 225$ K, the μ^+SR result supported the formation of a G-type AF ordered state with $\boldsymbol{M}_{\rm Cr} \parallel (001)$ at 2 K, as suggested by neutron diffraction measurements. However, $\boldsymbol{M}_{\rm Cr}$ was most likely to change its direction to (011) at temperatures above 10 K. The magnitude of $M_{\rm Cr}$ was estimated to be $2.1\mu_{\rm B}$ at both 2 and 50 K.

For the solid-solution system, $Ca_{1-x}La_xCu_3Cr_4O_{12}$, $T_{\rm N}$ and the internal magnetic field at 2 K increase monotonically with increasing x, as expected from the results for $CaCu_3Cr_4O_{12}$ and $LaCu_3Cr_4O_{12}$. In other words, the possibility of the existence of an eccentric phase in $Ca_{1-x}La_xCu_3Cr_4O_{12}$ was clearly excluded because the two end compounds are antiferromagnetic metals.

ACKNOWLEDGMENTS

We thank the staff of TRIUMF (especially the CMMS) for help with the μ^+SR experiments. All images involving crystal structure were made with VESTA [34]. M.I. was supported by Japan Society for the Promotion Science (JSPS) KAKENHI Grant No. JP24540362. M.M. was partly supported by Marie Skłodowska-Curie Action, International Career Grant through the European Commission and Swedish Research Council (VR), Grant No. INCA-2014-6426 as well as a VR neutron project grant (BIFROST, Dnr. 2016-06955). This work was supported by the Ministry of Education, Culture, Sports, Science and Technology (MEXT) of Japan, KAKENHI Grant No. JP23108003, and Japan Society for the Promotion Science (JSPS) KAKENHI Grant No. JP26286084.

APPENDIX

In order to further confirm the presence of the low-frequency component in the ZF-μ^+SR time spectrum for $CaCu_3Cr_4O_{12}$ below $T_{\rm N}$, Fig. 14 shows the Fourier transform frequency spectrum below 10 MHz, for which the Fourier transform was performed in the time range between 0 and 5 μs. Despite the different frequency range for the Fourier transform between Figs. 14 and 3(c), the result is very similar to that shown in Fig. 3(c). This clearly demonstrates the presence of the $A_{\rm AF_2}$ signal with $f_{\rm AF_2} \sim 2$ MHz below $T_{\rm N}$. A similar damped oscillation with $f_{\rm AF} \sim 1.5$ MHz was also found in Sr_2VO_4 [35].

[1] S. Doniach, Phys. B+C (Amsterdam, Neth.) **91**, 231 (1977).
[2] M. Subramanian, W. Marshall, T. Calvarese, and A. Sleight, J. Phys. Chem. Solids **64**, 1569 (2003).
[3] W. Kobayashi, I. Terasaki, J. Takeya, I. Tsukada, and Y. Ando, J. Phys. Soc. Jpn. **73**, 2373 (2004).
[4] J. Sugiyama, H. Nozaki, I. Umegaki, E. J. Ansaldo, J. H. Brewer, H. Sakurai, M. Isobe, and H. Takagi, Phys. Proc. **75**, 435 (2015).
[5] P. M. Woodward, Acta Crystallogr., Sect. B **53**, 32 (1997).
[6] P. M. Woodward, Acta Crystallogr., Sect. B **53**, 44 (1997).
[7] S. Tanaka, H. Takatsu, S. Yonezawa, and Y. Maeno, Phys. Rev. B **80**, 035113 (2009).
[8] S. Matar and M. Subramanian, Mater. Lett. **58**, 746 (2004).
[9] H. P. Xiang, X. J. Liu, E. J. Zhao, J. Meng, and Z. J. Wu, Inorg. Chem. **46**, 9575 (2007).
[10] M. Isobe, H. Sakurai, and H. Takagi, Meet. Abstr. Phys. Soc. Jpn. **69**, 386 (2014).
[11] S. Zhang, T. Saito, M. Mizumaki, and Y. Shimakawa, Chem. Eur. J. **20**, 9510 (2014).

[12] J. Sugiyama, M. Månsson, Y. Ikedo, T. Goko, K. Mukai, D. Andreica, A. Amato, K. Ariyoshi, and T. Ohzuku, Phys. Rev. B **79**, 184411 (2009).
[13] J. Sugiyama, H. Nozaki, M. Månsson, K. Prša, D. Andreica, A. Amato, M. Isobe, and Y. Ueda, Phys. Rev. B **85**, 214407 (2012).
[14] J. Sugiyama, H. Nozaki, K. Miwa, H. Yoshida, M. Isobe, K. Prša, A. Amato, D. Andreica, and M. Månsson, Phys. Rev. B **88**, 184417 (2013).
[15] J. Sugiyama, H. Nozaki, I. Umegaki, T. Uyama, K. Miwa, J. H. Brewer, S. Kobayashi, C. Michioka, H. Ueda, and K. Yoshimura, Phys. Rev. B **94**, 014408 (2016).
[16] A. Olariu, P. Mendels, F. Bert, B. G. Ueland, P. Schiffer, R. F. Berger, and R. J. Cava, Phys. Rev. Lett. **97**, 167203 (2006).
[17] A. Olariu, P. Mendels, F. Bert, L. K. Alexander, A. V. Mahajan, A. D. Hillier, and A. Amato, Phys. Rev. B **79**, 224401 (2009).
[18] F. Damay, C. Martin, V. Hardy, A. Maignan, G. André, K. Knight, S. R. Giblin, and L. C. Chapon, Phys. Rev. B **81**, 214405 (2010).
[19] F. Xiao, T. Lancaster, P. J. Baker, F. L. Pratt, S. J. Blundell, J. S. Möller, N. Z. Ali, and M. Jansen, Phys. Rev. B **88**, 180401 (2013).
[20] G. M. Kalvius, D. R. Noakes, and O. Hartmann, *Handbook on the Physics and Chemistry of Rare Earths* (North-Holland, Amsterdam, 2001), Vol. 32, Chap. 206, pp. 55–451.
[21] A. Yaouanc and P. D. de Réotier, *Muon Spin Rotation, Relaxation, and Resonance, Application to Condensed Matter* (Oxford University Press, New York, 2011).
[22] R. Kubo and T. Toyabe, *Magnetic Resonance and Relaxation* (North-Holland, Amsterdam, 1996).
[23] R. S. Hayano, Y. J. Uemura, J. Imazato, N. Nishida, T. Yamazaki, and R. Kubo, Phys. Rev. B **20**, 850 (1979).
[24] T. Saito, S. Zhang, D. Khalyavin, P. Manuel, J. P. Attfield, and Y. Shimakawa, Phys. Rev. B **95**, 041109 (2017).
[25] T. Sato, K. Miwa, Y. Nakamori, K. Ohoyama, H.-W. Li, T. Noritake, M. Aoki, S.-i. Towata, and S.-i. Orimo, Phys. Rev. B **77**, 104114 (2008).
[26] P. Hohenberg and W. Kohn, Phys. Rev. **136**, B864 (1964).
[27] W. Kohn and L. J. Sham, Phys. Rev. **140**, A1133 (1965).
[28] J. P. Perdew, K. Burke, and M. Ernzerhof, Phys. Rev. Lett. **77**, 3865 (1996).
[29] J. P. Perdew, K. Burke, and M. Ernzerhof, Phys. Rev. Lett. **78**, 1396 (1997).
[30] H. Kato, T. Tsuruta, M. Matsumura, T. Nishioka, H. Sakai, Y. Tokunaga, S. Kambe, and R. E. Walstedt, J. Phys. Soc. Jpn. **78**, 054707 (2009).
[31] K. M. Kojima, J. Yamanobe, H. Eisaki, S. Uchida, Y. Fudamoto, I. M. Gat, M. I. Larkin, A. Savici, Y. J. Uemura, P. P. Kyriakou *et al.*, Phys. Rev. B **70**, 094402 (2004).
[32] P. L. Russo, J. Sugiyama, J. H. Brewer, E. J. Ansaldo, S. L. Stubbs, K. H. Chow, R. Jin, H. Sha, and J. Zhang, Phys. Rev. B **80**, 104421 (2009).
[33] J. Sugiyama, K. Mukai, H. Nozaki, M. Harada, M. Månsson, K. Kamazawa, D. Andreica, A. Amato, and A. D. Hillier, Phys. Rev. B **87**, 024409 (2013).
[34] K. Momma and F. Izumi, J. Appl. Crystallogr. **44**, 1272 (2011).
[35] J. Sugiyama, H. Nozaki, I. Umegaki, W. Higemoto, E. J. Ansaldo, J. H. Brewer, H. Sakurai, T.-H. Kao, H.-D. Yang, and M. Månsson, Phys. Rev. B **89**, 020402(R) (2014).